High Molar Extinction Coefficient Ruthenium Sensitizers for Thin Film Dye-Sensitized Solar Cells

8 AUTHORS, INCLUDING:

Jun-Ho Yum
Centre Suisse d'Electronique et de Microte…
123 PUBLICATIONS **9,257** CITATIONS

Pawel Wagner
University of Wollongong
105 PUBLICATIONS **1,725** CITATIONS

Md Khaja Nazeeruddin
École Polytechnique Fédérale de Lausanne
490 PUBLICATIONS **45,107** CITATIONS

High Molar Extinction Coefficient Ruthenium Sensitizers for Thin Film Dye-Sensitized Solar Cells

Song-Rim Jang,[‡] Jun-Ho Yum,[†] Cedric Klein,[†] Kang-Jin Kim,[‡] Pawel Wagner,[§] David Officer,[§] Michael Grätzel,[†] and Mohammad K. Nazeeruddin*,[†]

Laboratory for Photonics and Interfaces, Institute of Chemical Sciences and Engineering, Ecole Polytechnique Fédérale de Lausanne, 1015 Lausanne, Switzerland

Received: September 1, 2008; Revised Manuscript Received: December 3, 2008

We present two sensitizers, Ru(4,4′-dicarboxyvinyl)-2,2′-bipyridine)(4,4′-dinonyl-2,2′-bipyridine)(NCS)$_2$ (K9) and Ru(4,4′-dicarboxy(phenylethenyl)-2,2′-bipyridine)(4,4′-dinonyl-2,2′-bipyridine)(NCS)$_2$ (K23), which were synthesized and characterized by analytical, spectroscopic, and electrochemical impedance measurements. The two sensitizers that contain hydrophobic alkyl chains and an extended π-conjugation bridge between carboxylic acid groups and the ruthenium chromophore center exhibit enhanced red response and higher molar extinction coefficients when compared to the Ru(4,4′-dicarboxy-2,2′-bipyridine)(4,4′-dinonyl-2,2′-bipyridine)(NCS)$_2$ (Z907) sensitizer. The performances of the K9, K23, and Z907 sensitizers in nanocrystalline TiO$_2$-based thin film solar cells were studied using transparent 2.6-μm-thick mesoporous layers, which show short-circuit photocurrent densities (J_{sc}) of 7.80, 8.31, and 7.16 mA/cm^2, corresponding to overall conversion efficiencies of 4.14, 4.41, and 4.06%, respectively. The increase in the J_{sc} of the cells with K9 and K23 with respect to that with Z907 is due to the enhanced molar extinction coefficient of the new sensitizers. The incident monochromatic photon-to-current conversion efficiency for the K23 is plotted as a function of excitation wavelength show in the plateau region 79% and even at 700 nm 69%.

Introduction

Dye-sensitized solar cells (DSSCs) are attracting widespread interest for the conversion of sunlight into electricity because of their low cost and high efficiency.[1−5] In these cells, the sensitizer is one of the key components, harvesting the solar radiation and converting it to electric current. Over the last 17 years, ruthenium complexes endowed with thiocyanate ligands have maintained a clear lead in performance among thousands of dyes that have been scrutinized. The pioneering studies on dye-sensitized solar cells using *cis*-dithiocyanatobis(4,4′-dicarboxylic acid-2,2′-bipyridine)ruthenium(II), (N3) is a paradigm in this field; the efficiency using relatively thick TiO$_2$ films under standard air mass 1.5 reporting conditions stands presently at 11%.[6−9] A new development for dyes applied to a solar cell comes from the preparation of an amphiphilic heteroleptic N3-equivalent, such as Z907 [RuLL′(NCS)$_2$] (L = 4,4′-dicarboxylic acid-2,2′-bipyridine; L′ = 4,4′-dinonyl-2,2′-bipyridine) in which the hydrophobic long chains interact laterally to form an aliphatic network to impede triiodide ions' reaching the TiO$_2$ surface.[10] To further improve the amphiphilic heteroleptic ruthenium sensitizers, we have developed high molar extinction coefficient dyes by expanding the π-conjugation of the hydrophobic ligand and endowing it with electron-donating alkoxy groups.[11−16] In these complexes, the anchoring carboxylic acid groups are substituted directly onto 2,2′-bipyridine.

In this paper, we report two novel sensitizers, Ru((4,4′-dicarboxyvinyl)-2,2′-bipyridine)(4,4′-dinonyl-2,2′-bipyridine)(NCS)$_2$ (K9) and Ru(4,4′-dicarboxy(phenylethenyl)-2,2′-bipyridine)(4,4′-dinonyl-2,2′-bipyridine)(NCS)$_2$ (K23), in which an extended π-conjugation is incorporated between the chromophore and the anchoring group. Incorporating either vinyl or phenylethenyl moieties into the anchoring bipyridine affords ruthenium sensitizers with increased molar extinction coefficients and enhanced red response in the visible regions.

Experimental Section

Analytical Measurements. UV/vis and fluorescence spectra were recorded in a 1 cm path length quartz cell on a Cary 5 spectrophotometer and Spex Fluorolog 112 spectrofluorometer, respectively. Electrochemical data were obtained by cyclic voltammetry in a conventional three-electrode cell with a PAR potentiostat. A glassy-carbon or a gold working electrode, platinum-wire auxiliary electrode, and saturated silver chloride electrodes were used in a single-compartment-cell configuration. ^{1}H and ^{13}C NMR spectra were measured on a Bruker 200 MHz spectrometer. The reported chemical shifts were in parts per million against TMS. The ATR-FTIR spectra for all the samples were measured using a Digilab 7000 FTIR spectrometer. The ATR data reported here were taken with the "Golden Gate" diamond anvil ATR accessory (Graseby-Specac) using typically 64 scans at a resolution of 2 cm^{-1}. The IR optical bench was flushed with dry air.

Materials. The solvents and reagents puriss grade quality were purchased from Fluka. 4,4′-Dinonyl-2,2′-bipyridine (dn-bpy), dichloro(*p*-cymene)ruthenium(II) dimer and potassium/ammonium thiocyanate were obtained (from Aldrich) and used as received. LH-20 Sephadex gel was obtained from Pharmacia. The intermediate product 4,4′-diformyl-2,2′-bipyridine, 4,4′-bis(carboxyvinyl)-2,2′-bipyridine ligand, and its heteroleptic

* Corresponding author. E-mail: mdkhaja.nazeeruddin@epfl.ch.
† Current address: Swiss Federal Institute of Technology.
‡ Current address: Department of Chemistry, Korea University, Seoul, Korea.
§ Current address: Intelligent Polymer Institute and Department of Chemistry, ARC Centre of Excellence for Electromaterials Science, University of Wollongong, Northfields Avenue, Wollongong, NSW 2522, Australia.

Ruthenium Sensitizers

J. Phys. Chem. C, Vol. 113, No. 5, 2009 **1999**

SCHEME 1: Synthetic Strategy for 4,4′-Dicarboxy(phenylethenyl)-2,2′-bipyridine
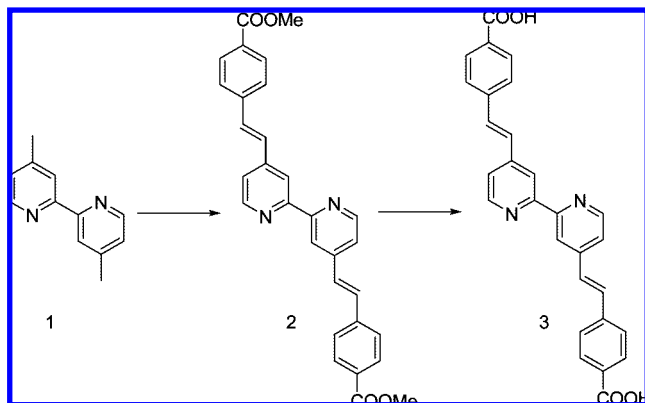
ruthenium complex (K9) were synthesized according to literature procedures.[13,14]

4,4′-Di(carboxyvinyl)-2,2′-bipyridine or 4,4′-Dicarboxy(phenylethenyl)-2,2′-bipyridine. 4,4′-Dimethyl-2,2′-bipyridine and methyl 4-formylbenzoate were purchased from Aldrich and Fluka, respectively. 4,4′-Di(phenylethenyl)-2,2′-bipyridine **3** was prepared by hydrolysis of the styryl ester **2**, which was synthesized from 4,4′-dimethyl-2,2′-bipyridine **1** by a modified version of the previously described procedure[17] as follows: 4,4′-dimethyl-2,2′-bipyridine (11.054 g, 0.06 mol) and methyl 4-formylbenzoate (29.549 g, 0.18 mol) were dispersed in acetic anhydride (16 mL), then dry potassium acetate (5.889, 0.06 mol) and iodine (50 mg, 2 × 10⁻⁴ mol) were added. The resulting mixture was heated under reflux for 48 h. After cooling, methanol (200 mL) was added, and the resulting fine off-white crystals were filtered off. The solid was stirred for 5 min with boiling methoxyethanol (400 mL), the mixture allowed to cool to RT, and the crystalline product was filtered off and dried to give pure styryl ester (19.449 g, 72%). The compound gave spectroscopic data identical to that previously reported. 4,4′-Dicarboxy(phenylethenyl)-2,2′-bipyridine **3** was then obtained in quantitative yield from the styryl ester according to the literature procedure.[17]

Ruthenium Complex K23. The complex K23 was synthesized by refluxing a mixture of 4,4′-dinonyl-2,2′-bipyridine (150 mg, 0.37 mmol) and dichloro(*p*-cymene)ruthenium(II) dimer (113 mg, 0.18 mmol) in argon-degassed absolute ethanol (40 mL) for 4 h. Evaporation of the solvent led to a dichloro(*p*-cymene)-4,4′-dinonyl-2,2′-bipyridine−ruthenium(II) complex as a brown-yellow oil in a quantitative yield. This intermediate complex was used without further purification for reacting with 4,4′-dicarboxy(phenylethenyl)-2,2′-bipyridine (0.36 mmol) in dry and argon-degassed DMF (30 mL). The mixture was heated at 150 °C for 4 h, and to the resulting dark purple solution was added NH₄NCS (408 mg, 5.4 mmol), and the mixture heated at 150 °C for an additional 4 h. After evaporation of the DMF, the resulting purple residue was suspended in water (200 mL) and sonicated for 5 min. The pH was adjusted to 3 with HNO₃ (0.02 M,) and the mixture was let stand in a refrigerator overnight. The crude complex was dissolved in methanol containing 2 equiv of tetrabutylammonium hydroxide. The concentrated solution was filtered through a sintered glass crucible and charged onto an LH-20 Sephadex column, which was prepared in methanol. The adsorbed complex was eluted using methanol as an eluent. The main band was collected, and the solution pH was lowered to 3 using 0.02 M HNO₃ acid. The precipitated complex was collected on a glass frit and air-dried: yield 60 mg, 32%. The analytical and spectroscopic data are consistent with the structures shown in Figure 1.

Preparation of Mesoscopic TiO₂ Films. Fluorine-doped SnO₂ conducting (FTO) glass plates (Nippon Sheet Glass, 4 mm thick, 8 Ω/sq) were cleaned in a detergent solution, rinsed with water and ethanol, and then treated in a UV−O₃ system for 20 min to remove organics or contamination. The cleaned plates were treated with a 40 mM TiCl₄ aqueous solution at 70 °C for 30 min to facilitate a good mechanical contact between the following printed TiO₂ layer and the conducting glass matrix. Next, the transparent film of 20 nm TiO₂ particles was screen-printed on the treated conducting glass.[7,18] A thicker transparent TiO₂ layer can be obtained by repeating the screen printing operation. In this research, 2.6- and 4.4-μm-thickness films as the transparent film and 1.8-, 2.5-, 5.5-, 7.0-, and 10-μm-thickness films as the double-layer films were used. A 4−5 μm
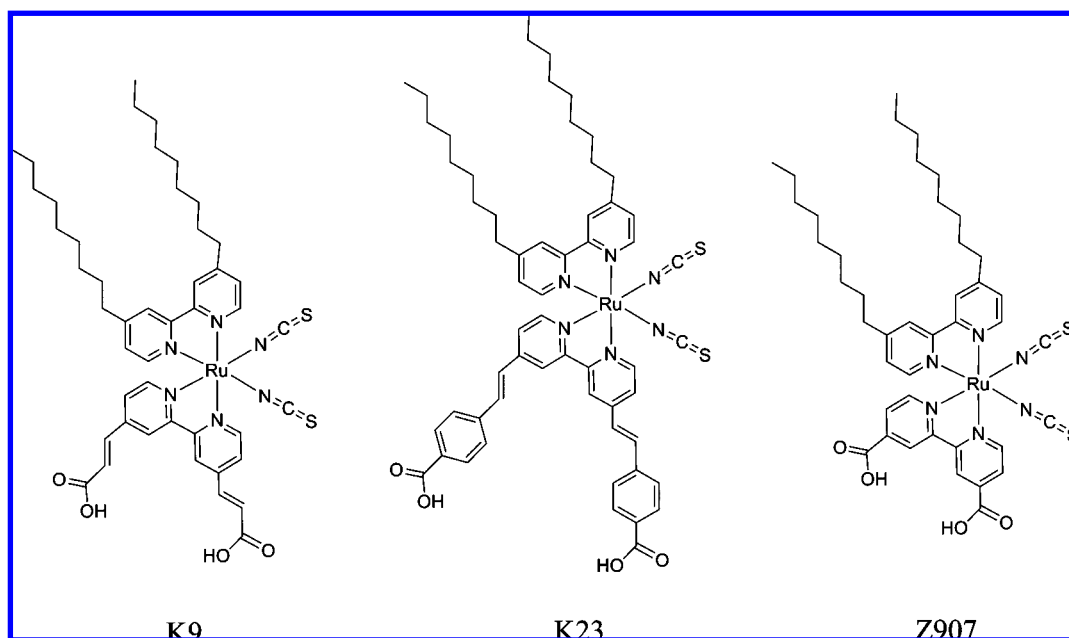

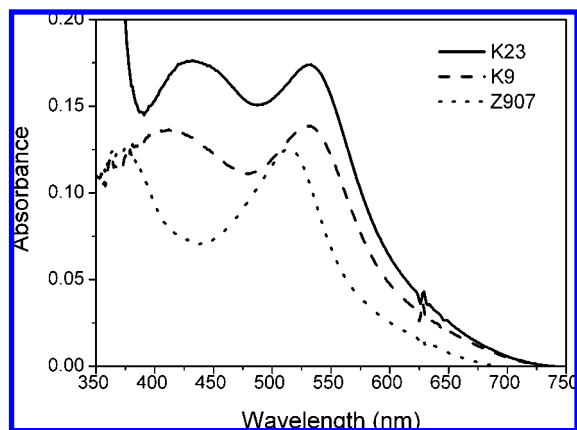**Figure 1.** Molecular structures of K9, K23, and Z907 sensitizers.

2000 *J. Phys. Chem. C, Vol. 113, No. 5, 2009*

Jang et al.

Figure 2. UV−vis spectra of 1×10^{-5} M each of Z907, K9, and K23 sensitizers in EtOH.

TABLE 1: Comparison of Absorption Peaks and Molar Absorption Coefficients of the Synthesized Sensitizers K9 and K23 with Z907[a]

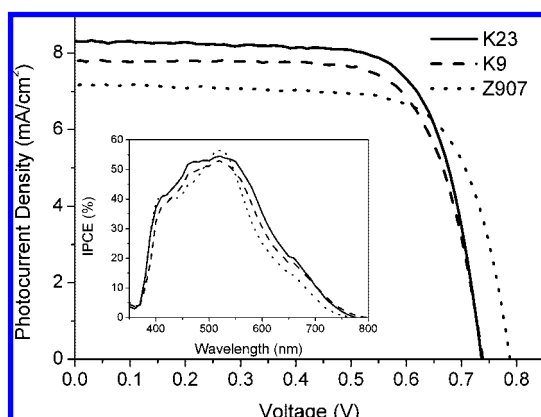| sensitizer	λ_{max} (nm) (ε_{max} (10^4 M^{-1} cm^{-1}))
Z907	375 (1.24), 515 (1.26)
K9	413 (1.35), 530 (1.38)
K23	433 (1.75), 533 (1.74)

[a] Measured in ethanol.

Figure 3. $J-V$ curves of DSSCs prepared with TiO$_2$ films impregnated with Z907, K9, and K23 sensitizers in acetonitrile and *tert*-butyl alcohol (volume ratio = 1:1). Light intensity was 100 mW/cm^2. The inset shows the corresponding IPCE spectra.

TABLE 2: Photovoltaic Parameters of the Dye-Sensitized Solar Cells with Different Sensitizers[a]

sensitizer	J_{sc} (mA/cm^2)	V_{oc} (mV)	FF	η (%)	thickness (μm)[b]
Z907	7.16	787.82	0.720	4.06	2.6
K9	7.80	738.23	0.719	4.14	
K23	8.31	736.14	0.722	4.41	
Z907	15.09	700.86	0.682	7.18	2.5 + 5
K9	15.16	693.26	0.658	6.92	
K23	15.73	707.71	0.669	7.45	

[a] Measured under an illumination of AM 1.5 solar light (100 mW/cm^2). [b] The second number indicates the thickness of the scattering layer.

light-scattering layer of 400 nm anatase particles (CCIC, HPW-400) was also coated on the transparent films The electrodes coated with the TiO$_2$ pastes were gradually heated under an air flow at 325 °C for 5 min, at 375 °C for 5 min, at 450 °C for 15 min, and at 500 °C for 15 min. These electrodes were again treated with TiCl$_4$ and heated to 70 °C for 30 min.
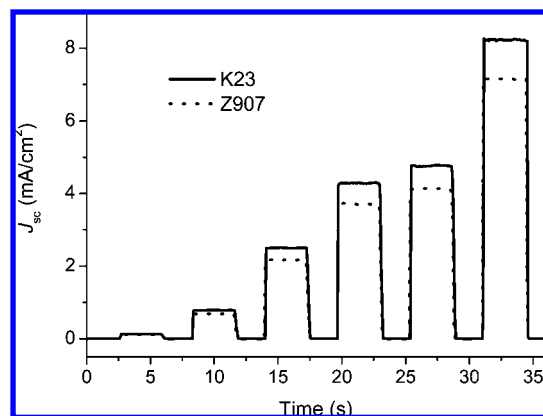

Figure 4. The current dynamics transient spectra of DSSC devices with Z907 and K23 sensitizers under various light intensities.
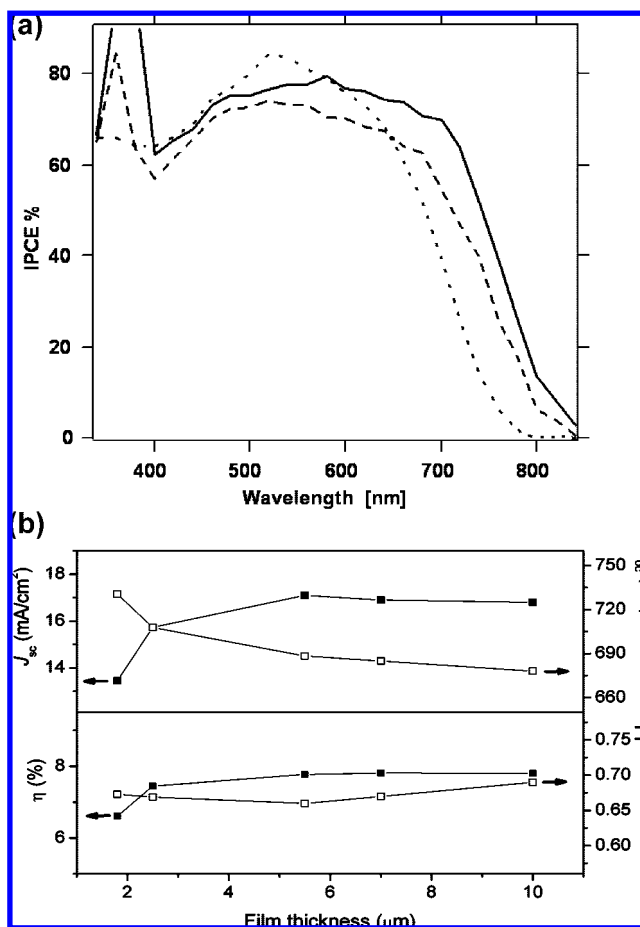

Figure 5. (a) Photocurrent action spectrum obtained with Z907 (dotted line), K9 (dashed line), and K23 (solid line) sensitizers attached to thick nanocrystalline TiO$_2$ film (12 + 5 μm). The incident photon-to-current conversion efficiency is plotted as a function of the wavelength of the exciting light using an electrolyte consisting of 0.6 M 1-butyl-3-methyl imidiazolium iodide (BMII), 0.05 M iodine (I$_2$), 0.1 M LiI, and 0.5 M *tert*-butylpyridine (TBP) in a mixture of acetonitrile/valeronitrile (85:15,v/v). (b) Film thickness dependence of J_{sc}, V_{oc}, fill factor, and efficiency of DSSCs for K23-coated electrodes.

Fabrication of Dye-Sensitized Solar Cells. After a sintering at 500 °C for 30 min followed by cooling to ∼80 °C, they were immersed into the dye solution at room temperature for 17 h. The sensitizing dye solution contained 0.3 mM K9 or K23 in acetonitrile and *tert*-butyl alcohol (volume ratio = 1:1). The counter electrodes were prepared by coating an FTO plate (TEC 15, 2.2 mm thickness, Libbey-Owens-Ford Industries) with a
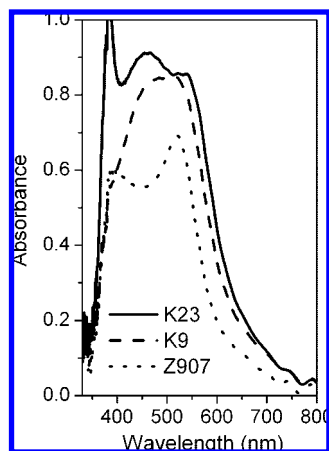
Ruthenium Sensitizers

J. Phys. Chem. C, Vol. 113, No. 5, 2009 **2001**

Figure 6. UV−vis spectra of 3.5-μm-thick TiO$_2$ films coated with Z907, K9 and K23 in MeCN/*t*BuOH.

drop of H$_2$PtCl$_6$ solution (2 mg of Pt in 1 mL of ethanol) and heating it at 430 °C for 15 min. The dye-coated TiO$_2$ electrode and Pt counter electrode were assembled into a sealed sandwich-type cell by heating with a hot-melt ionomer film (Surlyn 1702, 25 μm thickness, Du-Pont) as a spacer between the electrodes. A drop of the electrolyte solution that consists of 0.6 M 1-butyl-3-methyl imidiazolium iodide (BMII), 0.05 M iodine (I$_2$), 0.1 M LiI, and 0.5 M *tert*-butylpyridine (TBP) in a mixture of acetonitrile/valeronitrile (85:15,v/v) labeled as A7117 was incorporated as in the previously described method.[7,18]

Measurements. For photocurrent−voltage measurements of the DSSCs, the irradiation source was a 450 W xenon light source (Osram XBO 450, U.S.A.), whose power was equivalent to an AM 1.5 solar simulator and was calibrated by using a Tempax 113 solar filter (Schott). The output power of the AM 1.5 solar simulator was calibrated by using a reference Si photodiode equipped with a colored matched IR-cutoff filter (KG-3, Schott) to reduce the mismatch in the region of 350−750 nm between the simulated light and AM 1.5 to <2%. The measurement delay time of photo I−V characteristics of DSCs was fixed to 40 ms. The measurement of incident photon-to-current conversion efficiency was plotted as a function of excitation wavelength by using the incident light from a 300 W xenon lamp (ILC Technology, U.S.A.), which was focused through a Gemini-180 double monochromator (Jobin Yvon Ltd.).

Photogenerated transients were observed by using an exciting pulse generated by red-light-emitting diodes with a white light bias. Photovoltage transients were observed by using a pump pulse generated by four red-light-emitting diodes controlled by a fast solid-state switch. Pulse widths of 50 ms were used, with a rise and fall time of ≤2 μs. The pulse of red light was incident on the photoanode side of the cell, and its intensity was controlled to keep the modulation of the voltage below 10 mV. The bias light was incident on the same side and was attenuated when needed by changing power. From the current decay, the photogenerated charge in the cell is measured. The corresponding voltage decay gives the electron lifetime.

Desorption of dyes was effected from 0.27 cm^2 TiO$_2$ films (2.5 + 5 μm) into 3 mL of 10 mM tetrabutyl ammonium hydroxide (TBAOH) in ethanol.

Results and Discussion

Figure 2 shows UV−vis absorption spectra of 1 × 10^{-5} M for each of the K9 and K23 sensitizers, as compared with the Z907 sensitizer in ethanol. The absorption spectra of the K9 and K23 sensitizers are dominated by metal-to-ligand charge transfer transitions (MLCT), which are located at 413 and 530 nm and 433 and 533 nm, respectively (Table 1). The peak positions of the lowest-energy MLCT band of the K9 and K23 sensitizers are red-shifted by 15 and 18 nm, respectively, when compared with the Z907 sensitizer, and the molar extinction coefficients at the peak wavelengths of the new sensitizers are higher by 15 and 38%, respectively. The increased π-conjugation lengths of 4,4′-bis(carboxyvinyl)-2,2′-bipyridine in K9 and 4,4′-bis((carboxyphenyl)ethenyl)-2,2′-bipyridine in K23 are responsible for the increased molar extinction coefficients in the visible region, as compared with the Z907 sensitizer. The high-energy bands below 350 nm are due to ligand $\pi-\pi^*$ transitions.

Figure 3 shows a comparison of the photocurrent−voltage ($J-V$) curves and the incident photon-to-current conversion efficiency spectra of the dye-sensitized solar cells consisting of the three dyes Z907, K9, and K23 sensitizers. For the $J-V$ and IPCE measurements, we used TiO$_2$ films consisting of a transparent 2.6-μm-thick mesoporous thin film to compare the effects of sensitizers in the DSSC. The $J-V$ data indicate that the photocurrents of the K9- and K23-coated TiO$_2$ cells are higher than that of Z907, whereas the open circuit potentials are lower than that of Z907. The short-circuit photocurrent density (J_{sc}) of the TiO$_2$ cell with K23 sensitizer has increased by 16%, and the open-circuit voltage (V_{oc}) of that has decreased by 6.6% as compared with Z907. As a result, the overall solar energy conversion efficiency of the K23-sensitized cell increased by 8.6%. The J_{sc} values of K9, K23, and Z907 are consistent with the IPCE values, as shown in the inset of Figure 3. In addition, the cells consisting of K9 and K23 sensitizers show consistently broad IPCE spectra compared with that of Z907. The enhanced IPCE values correspond to the increased absorptions in the visible and near-IR spectral region.

The corresponding photovoltaic data, the short-circuit photocurrent density (J_{sc}), open-circuit voltage (V_{oc}), fill factor (FF), and solar-to-electricity conversion efficiency (η) values, when using each sensitizer and adding a scattering layer of 5 μm thickness, are summarized in Table 2. Notably, the J_{sc} for all sensitizers doubled upon adding a scattering layer.

In addition, we obtained the current dynamics transient spectra of DSSCs based on the K23 and Z907 under various light intensities, which were recorded in a light on−off sequence produced by opening and closing a mechanical shutter that blocks the light beam (Figure 4). Under all light intensities, the photocurrents of the TiO$_2$ cell with K23 sensitizer increased by ∼16% in comparison with Z907.

Figure 5a presents photocurrent action spectra of the Z907, K9, and K23 sensitizers obtained with a thick TiO$_2$ film composed of a 12 μm transparent layer and a 5 μm scattering layer. The incident monochromatic IPCE plotted as a function of excitation wavelength shows 79% in the plateau region for the K23 sensitizer. Strikingly, the incident monochromatic photon-to-current conversion efficiency, even at 700 nm for K23 sensitizer, is 69%. The enhanced red response of the K23 sensitizer compared to the Z907 complex is consistent with the absorption spectra of these two sensitizers. Figure 5b presents the photovoltaic data of DSSCs with TiO$_2$ films sensitized with K23 of varying thicknesses (1.8, 2.5, 5.5, 7, and 10 μm) with a 5 μm scattering layer. The data were obtained with averaged values of two cells for each condition. The data reveals that the V_{oc} decreases with increasing film thickness, which is likely due to the increased surface area of the TiO$_2$ film that provides additional charge-recombination sites, enhancing the dark cur-
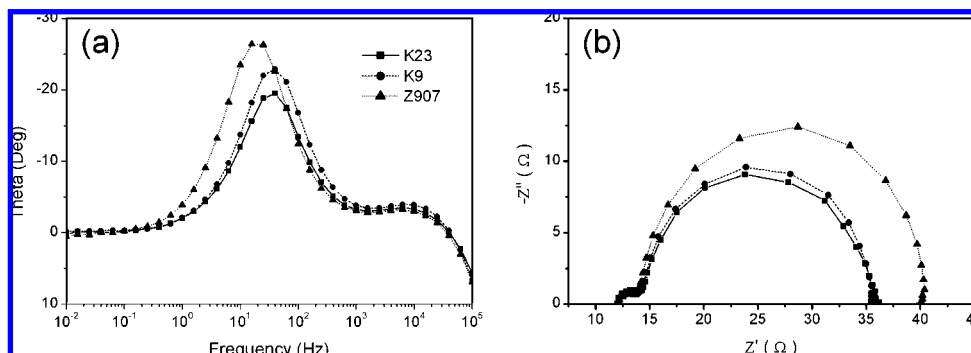
2002 *J. Phys. Chem. C, Vol. 113, No. 5, 2009*

Jang et al.

Figure 7. Impedance spectra of Z907, K9, and K23 DSSCs based on $1.8 + 4$ μm film thickness measured under 1 sun at open circuit potential. (a) Bode phase plots and (b) Nyquist plots. Electrolyte A7117 was used.

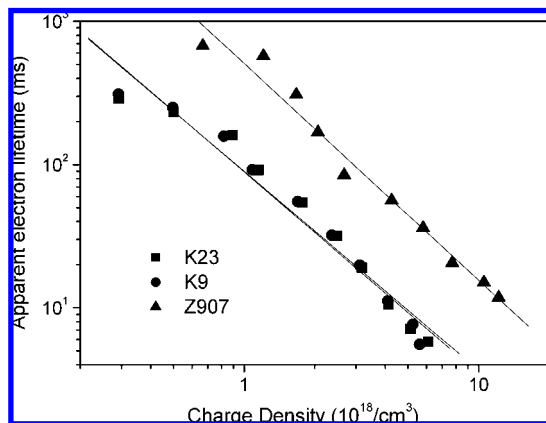**Figure 8.** Plot of apparent electron lifetime against photoinduced charge density of Z907, K9, and K23 DSSCs with a 4.4 μm TiO$_2$ film thickness. Electrolyte A7117 was used.
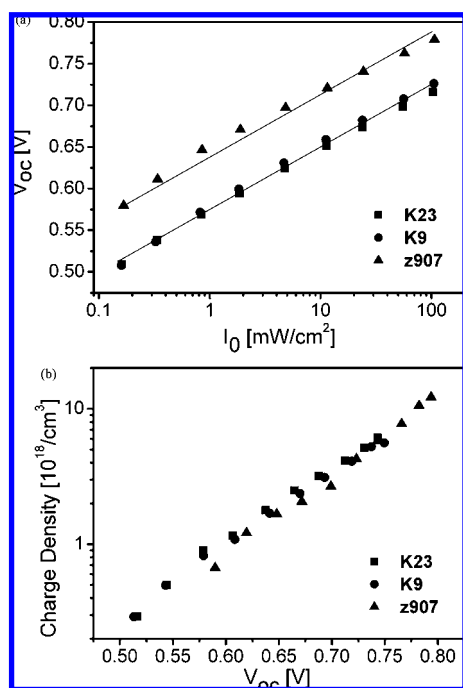

Figure 9. Open circuit voltage against incident light intensity (a) and photoinduced charge density against open circuit voltage (b) of Z907, K9, and K23 DSSCs based on 4.4 μm TiO$_2$ film thickness. Electrolyte A7117 was used.

rent. Moreover, for thicker films, the sensitizers on the outer TiO$_2$ particle layers do not contribute significantly to the photogeneration of electrons due to the filtering of photons by

the sensitized particles located close to the FTO glass, and thus, the J_{sc} is almost saturated from ∼7 μm. The sharing of photoinjected electrons through conduction bands by these particles lowers their quasi-Fermi level and, hence, the V_{oc}.[12] As shown in Figure 5, the conversion efficiency (η) for the cell with K23 is observed to be saturated from $7 + 5$ μm film thickness. The K9 sensitizer also shows a similar trend that the V_{oc} decreases and the J_{sc} increases as a function of the thickness of the films.

To investigate dye loading on TiO$_2$ films, we used the UV−vis absorption spectra of the dye-coated 3.5-μm-thick TiO$_2$ films and measured the dye concentration by desorbing it from 2.5- + 5-μm-thick TiO$_2$ films. Figure 6 clearly shows that the optical density of the K9- and K23-derivatized TiO$_2$ films is higher over the entire spectral region as compared to that of Z907. Using the molar absorption coefficients at maximum wavelengths in Table 1, the concentration of Z907, K9, and K23 desorbed from their TiO$_2$ films was found to be 3.21×10^{-6}, 3.48×10^{-6}, and 3.43×10^{-6} M, respectively, indicating that dye loadings of K9 and K23 are the same as Z907. On the basis of the concentration, we calculated the moles of sensitizers adsorbed to the unit area of TiO$_2$ films and found 3.47×10^{-8}, 3.88×10^{-8}, and 3.74×10^{-8} mol/cm^2, respectively, for Z907, K9, and K23. Since the surface coverage of all the sensitizers is similar, the higher absorbance of K9 and K23 compared to Z907 must be caused by their higher light-harvesting ability (higher molar extinction coefficient).

Electrochemical impedance spectroscopy (EIS) provides valuable information for the understanding and characterization of the basic photovoltaic parameters of the DSSC. The physical models and equivalent circuits associated with this experimental technique have been applied to the analysis of the electron recombination at the TiO$_2$/electrolyte interface, electron transport in the TiO$_2$ electrode, electron transfer at the counter electrode, and I$_3^-$ transport in the electrolyte phase of DSSCs.[9,19−21] We have measured the electrochemical impedance spectra of DSSCs with Z907, K9, and K23 sensitizers at open-circuit voltage under the conditions of 1 sun (Figure 7). At open circuit voltage under illumination, as the oxidized dye is regenerated by I$^-$, the absorbed photon energy is converted through the two coupled redox cycles involving sensitized electron injection, dye regeneration, and electron recapture by I$_3^-$. Consequently, there is no net current flowing through the cell under illumination.[21] In Figure 7, the large semicircle in the Nyquist plot and the characteristic frequency peak in the Bode phase plot arise from electron transfer at the TiO$_2$/electrolyte interface (electron transfer from the conduction band of the mesoscopic film to triiodide ions in the electrolyte). The frequency peaks from the K9 and K23 DSSCs in the Bode phase plots (Figure 7a) are at

Ruthenium Sensitizers

J. Phys. Chem. C, Vol. 113, No. 5, 2009 **2003**

higher frequencies than that from the Z907 DSSC, indicating that the electron lifetimes of the K9 and K23 sensitizers are shorter than that of the Z907 sensitizer. This can be ascribed to a decrease in the electron diffusion length.[12] This trend can also be seen in the Nyquist plots (Figure 7b) with corresponding reductions in the radii of the semicircles. The impedance is due to electron transfer from the conduction band of the TiO_2 film to triiodide ions in the electrolyte, represented by the radius of the semicircle. This impedance from the K dye-sensitized solar cells is evidence that the recombination process is faster than the Z907 sensitizer, leading to the lower photovoltages of K dyes cells. The increased photocurrents of the K9 and K23-sensitized cells with the thin TiO_2 films can be explained by the high molar extinction coefficients of these sensitizers as compared with Z907.

Figure 8 shows the relationship between apparent electron lifetime in the DSSCs as a function of photoinduced charge density. The two K-sensitized cells have similar but shorter electron lifetimes than the Z907-coated cell. When these data were fitted, the electron lifetimes in the Z907-sensitized and two K-sensitized solar cells were found to be 497 and 91 ms, respectively, at a charge density of 1×10^{18} cm^{-3} and at a fixed photoinduced charge. At a higher charge density, 5×10^{18} cm^{-3}, the electron lifetimes were 45 and 9 ms for Z907- and K-sensitized solar cells, respectively. This indicates that the electron lifetimes of the K-sensitized solar cells are about 5 times shorter than that of Z907, which can presumably be correlated to the closeness of the carboxylic acid groups to the ruthenium center in the chemical structure (Figure 1). This result is in agreement with the impedance result discussed above. Since K9 and K23 sensitizers have distantly connected carboxylic acids to bipyridyl groups compared with a direct connection in the case of the Z907, the electrons generated in K-sensitized solar cells can be recombined with triiodide at the TiO_2/electrolyte interface.

Finally, we obtained the data of photoinduced charge densities against the open circuit voltage and short circuit current density of Z907, K9, and K23 DSSCs to understand the decreased V_{oc} by the two K sensitizers. To obtain V_{oc} and J_{sc} as a function of charge densities, photocurrent–voltage measurement was performed at various intensities of light, inducing different charge densities before photogenerated transient measurement. Hence, V_{oc} and J_{sc} corresponding to different charge densities could be obtained and plotted in Figure 9. Figure 9a shows the logarithmic dependence of V_{oc} on the incident light power, I_0 over a range of 0.1–100 mW/cm^2. All slopes are the same, which suggests that the mechanism of back-electron-transfer is not changed as different dyes incorporate the different lengths of the anchoring group. Figure 9b shows the differences in the photoinduced charge density among Z907, K9, and K23 sensitized solar cells as a function of the open circuit. A higher V_{oc} at a constant photoelectron density indicates upward movement of the conduction band edge, and conversely, a lower V_{oc} indicates a downward shift of the conduction band edge inasmuch as photoinduced electron density solely determines the difference between the conduction band edge and the electron quasi-Fermi level under illumination.[22] The V_{oc} values of the two K-sensitized solar cells at the same photoinduced charge density are slightly lower than that of the Z907-sensitized cell. Hence, the decreased V_{oc} of K9- and K23-sensitized cells in Figure 3 can be explained by faster recombination than that of Z907 and by a small influence of the band edge shift.

Conclusions

We have designed and synthesized two new ruthenium sensitizers, K9 and K23, with conjugated linkers on the anchoring bipyridyl group. This enables enhancements in the short-circuit photocurrents in thin film DSSCs as compared with Z907 dye-sensitized cells due to increased molar extinction coefficients and enhanced spectral response in the visible light and the near-IR regions. The new sensitizers show short electron lifetime and fast recombination; as a result, the DSSCs with the new sensitizers show decreased open-circuit voltage. However, the increase in J_{sc} more than offsets the decrease in V_{oc}, resulting in an overall increase in solar energy conversion efficiency for thin film DSSCs as compared with that of Z907 under air mass 1.5 sunlight.

References and Notes

(1) O'Regan, B.; Grätzel, M. *Nature* **1991**, *353*, 737.

(2) Nazeeruddin, M. K.; Kay, A.; Rodicio, I.; Humphry-Baker, R.; Müller, E.; Liska, P.; Vlachopoulos, N.; Grätzel, M. *J. Am. Chem. Soc.* **1993**, *115*, 6382.

(3) Hagfeldt, A.; Grätzel, M. *Chem. Rev.* **1995**, *95*, 49.

(4) Hagfeldt, A.; Grätzel, M. *Acc. Chem. Res.* **2000**, *33*, 269.

(5) Grätzel, M. *Nature* **2001**, *414*, 338.

(6) Grätzel, M. *J. Photochem. Photobiol., A* **2004**, *164*, 3.

(7) Nazeeruddin, M. K.; Pechy, P.; Renouard, T.; Zakeeruddin, S. M.; Humphry-Baker, R.; Comte, P.; Liska, P.; Cevey, L.; Costa, E.; Shklover, V.; Spiccia, L.; Deacon, G. B.; Bignozzi, C. A.; Grätzel, M. *J. Am. Chem. Soc.* **2001**, *123*, 1613.

(8) Wang, Z.-S.; Yamaguchi, T.; Sugihara, H.; Arakawa, H. *Langmuir* **2005**, *21*, 4272.

(9) Nazeeruddin, M. K.; De Angelis, F.; Fantacci, S.; Selloni, A.; Viscardi, G.; Liska, P.; Ito, S.; Bessho, T.; Grätzel, M. *J. Am. Chem. Soc.* **2005**, *127*, 16835.

(10) Zakeeruddin, S. M.; Nazeeruddin, M. K.; Humphry-Baker, R.; Pechy, P.; Quagliotto, P.; Barolo, C.; Viscardi, G.; Grätzel, M. *Langmuir* **2002**, *18*, 952.

(11) Kroon, J. M.; Bakker, N. J.; Smit, H. J. P.; Liska, P.; Thampi, K. R.; Wang, P.; Zakeeruddin, S. M.; Grätzel, M.; Hinsch, A.; Hore, S.; Wüfel, U.; Sastrawan, R.; Durrant, J. R.; Palomares, E.; Pettersson, H.; Gruszecki, T.; Walter, J.; Skupien, K.; Tulloch, G. E. *Prog. Photovoltaics* **2007**, *15*, 1.

(12) Kuang, D.; Ito, S.; Wenger, B.; Klein, C.; Moser, J.; Humphry-Baker, R.; Zakeeruddin, S. M.; Grätzel, M. *J. Am. Chem. Soc.* **2006**, *128*, 4146.

(13) Kuang, D.; Klein, C.; Ito, S.; Moser, J.-E.; Humphry-Baker, R.; Evans, N.; Duriaux, F.; Grätzel, C.; Zakeeruddin, S. M.; Grätzel, M. *Adv. Mater.* **2007**, *19*, 1133.

(14) Jang, S.-R.; Lee, C.; Choi, H.; Ko, J.; Lee, J.; Vittal, R.; Kim, K.-J. *Chem. Mater.* **2006**, *18*, 5604.

(15) Lagref, J.-J.; Nazeeruddin, M. K.; Grätzel, M. *Synth. Met.* **2003**, *138*, 333.

(16) Klein, C.; Nazeeruddin, M. K.; Liska, P.; Di Censo, D.; Hirata, N.; Palomares, E.; Durrant, J. R.; Grätzel, M. *Inorg. Chem.* **2005**, *44*, 178.

(17) Balasubramanian, K. K.; Cammarata, V.; Wu, Q. *Langmuir* **1995**, *11*, 1658.

(18) Wang, P.; Zakeeruddin, S. M.; Comte, P.; Charvet, R.; Humphry-Baker, R.; Grätzel, M. *J. Phys. Chem. B* **2003**, *107*, 14336.

(19) Bisquert, J. *J. Phys. Chem. B* **2002**, *106*, 325.

(20) Fabregat-Santiago, F.; Bisquert, J.; Garcia-Belmonte, G.; Boschloo, G.; Hagfeldt, A. *Sol. Energy Mater. Sol. Cells* **2005**, *87*, 117.

(21) Wang, Q.; Moser, J.-E.; Grätzel, M. *J. Phys. Chem. B* **2005**, *109*, 14945.

(22) Kopidakis, N.; Neale, N. R.; Frank, A. J. *J. Phys. Chem. B* **2006**, *110*, 12485.